DOI: 10.1002/((please add manuscript number))
Article type: Communication

Photothermally Responsive Inks For Inkjet-Printing Secure Information

Giuseppe Chirico, Giacomo Dacarro, Colm O'Regan, Jouko Peltonen, Jawad Sarfraz, Angelo Taglietti, Mykola Borzenkov, and Piersandro Pallavicini**

Dr. M. Borzenkov
Dipartimento di Medicina e Chirurgia and Nanomedicine Center, Università di Milano-Bicocca, piazza dell'Ateneo Nuovo, 20126, Milano, Italy;
Prof. G. Chirico
Dipartimento di Fisica and Nanomedicine Center, Università di Milano-Bicocca, piazza dell'Ateneo Nuovo, 20126, Milano, Italy; CNR - ISASI, Institute of Applied Sciences & Intelligent Systems, Via Campi Flegrei 34, Pozzuoli, NA, Italy
E-mail: mykola.borzenkov@unimib.it
Prof. G. Dacarro, A. Taglietti, P. Pallavicini
Dipartimento di Chimica, Università di Pavia, viale Taramelli, 12, 27100 Pavia, Italy
E-mail: piersandro.pallavicini@unipv.it
Dr. Colm O'Regan
King Abdullah University of Science and Technology (KAUST), Biological and Environmental Science and Engineering (BESE) Division, NABLA Lab, 23955-5900 Thuwal, Saudi Arabia
Dr. J. Peltonen
Laboratory of Physical Chemistry, Center for Functional Materials, Åbo Akademi University, Porthaninkatu 3-5, 20500, Turku, Finland
Dr. J. Sarfraz,
Nofima—Norwegian Institute of Food, Fisheries and Aquaculture Research, P.O. Box 210, NO-1431 Ås, Norway and Laboratory of Physical Chemistry, Center for Functional Materials, Åbo Akademi University, Porthaninkatu 3-5, 20500, Turku, Finland

Keywords: nanoinks, gold nanostars, secure information, inkjet printing, photothermal effect

Abstract. 2D patterns of photothermally responsive Near-Infrared (NIR) absorbing gold nanostars (GNS), coated with multiple charged polymer layers, have been inkjet-printed on a glass surface. The shape of the LSPR NIR absorption bands in the printed patterns looses its peaked form due to plasmon coupling, unless GNS are enveloped in multiple coating layers, keeping the inter-GNS distance sufficiently large. In the latter case, the photo-thermal temperature increase (ΔT) induced by the NIR laser irradiation follows a ΔT vs irradiation wavelength (λ_{irr}) profile with the same sharply peaked shape of the LSPR bands of the liquid ink. With this result, a new paradigm for inkjet-writing secure information is introduced, as an alternative to the current methods based on direct visual inspection of printed patterns. While the

printed ink patterns of GNS with different coatings are visually indistinguishable despite their different NIR absorption spectrum, their photothermal response changes dramatically with λ_{irr}. This allows either to write and read simple information using a single λ_{irr} (YES answer for $\Delta T >$ threshold) or to use multiple λ_{irr} to write and read complex information like thermal barcodes and anti-counterfait signatures.

Text. 2D-inkjet printing has been applied to pattern materials such as circuits, transistors, conductive polymers, ceramics[1,2] and biomaterials,[3] eg for sensing and scaffolding cell growth.[4-9] Inks made of colloidal solutions of nanoparticles (NP) may be particularly interesting, due to the additional physical-chemical features brought by the nanoscale[1,10] In this context, we have recently shown[11] that inks based on colloidal solutions of PEGylated gold nanostars (GNS) can be inkjet-printed on coated paper. GNS are NP with 3-6 sharp branches protruding from a core, displaying multiple intense LSPR absorption bands, whose maxima can be tuned in the 750-1800 nm range depending on the synthetic conditions.[12-14] These LSPR bands are photothermally active[12,15-18] and when irradiated (typically with a laser source) generate a local T increase. We have already shown that in a colloidal solution of GNS the observed T increase, ΔT, is a function of the laser fluence (I_{exc}, W/cm^2), of the GNS concentration and of the irradiation wavelength (λ_{irr}).[19] In particular, as pictorially sketched in **Figure 1A**, at a given I_{exc} the largest ΔT values (vertical bars) are observed when $\lambda_{irr} = \lambda_{max}$, where λ_{max} is the wavelength of maximum GNS absorption (a typical absorption spectrum of GNS in solution is displayed on the left back panel). In solution, the ΔT vs λ_{irr} output has thus the same peaked trend of the LSPR bands.[12,19] Also the patterns of GNS inks printed on coated paper[11] maintain a photothermal activity. The ΔT values were measured in a straightforward experimental setup using a commercially available thermo-camera, finding 20-80 °C ΔT by laser-irradiating at 800 nm with $0.2 < I_{exc} < 0.8$ W/cm^2. Such study was carried out to promote the

release of thiolated molecules grafted on the printed GNS surface by switching the local temperature.[11]

With this background we introduce here a new paradigm for inkjet-writing secure information, that we believe can be used as an alternative to the current secure writing methods, that are based on direct visual inspection of codes obtained with complex technologies (eg holography). The founding idea is that if a laser-irradiated printed pattern of a GNS ink presented a peak-like ΔT vs λ_{irr} profile as in solution, such printed pattern could be interrogated with laser sources at different λ_{irr} and different I_{exc}. A YES answer would be obtained if a ΔT larger than a chosen threshold value is read (eg with a thermocamera). As an example, in the scheme of Figure 1,A such ΔT value is 16 °C. As evidenced by the horizontal azure plane, in this hypothetical system only λ_{irr} = 1460 nm with I_{exc} = 1.0 W/cm^2 or 1.5 W/cm^2 would give a photothermal YES answer. It is noteworthy that the visual appearance of a printed GNS ink pattern is blue-black, independently on the band structure of their NIR absorption spectrum, so no further information is provided to a reader without photothermal interrogation. Even in this simple scheme, the code for reading a YES thermal answer can be hidden in a variety of parameters, such as the ink features (the shape of the GNS absorption spectrum, the wavelength of their LSPR) as well as the laser λ_{irr} and I_{exc}, and the mass of GNS be printed on a surface unit i.e. ink concentration and inkjet printing parameters.

To develop such approach for printing secure information, it is mandatory to ascertain that the band-structured absorption spectrum of GNS in the liquid ink is kept also in a dry printed pattern. To investigate this we first prepared a colloidal solution of GNS and coated them with HS-PEG_{2000} (mw 2000), obtaining GNS|PEG aqueous solutions according to the standard procedures used in our laboratories[12,13] (see details in the SI), with 0.6 μg/mL Au concentration as determined by ICP-OES analysis and particle size xx nm. This GNS|PEG colloidal solution had a blue-black color and displayed an absorption spectrum with a LSPR NIR band at 810 nm, Figure 1B, blue line. We prepared an ink by diluting this solution 2:1 v/v with 2-propanol to

adjust the viscosity and surface tension to suitable values for inkjet printing.[11] We printed this ink on flat microscopy cover glasses (2.1x2.6 cm), under ambient conditions using a single nozzle with drop volume 10 pL, firing voltage 27 ± 3 V, drop spacing 25 and a custom waveform to ensure optimal droplet formation. The dimensions of the produced printed film was 1x1 cm. Monolayer and multilayers (up to 11 layers) were printed to obtain films with increasing print density as shown in table…SI (here may be you can add the table I sent yesterday) (see SI for full details and a photography of the slides).

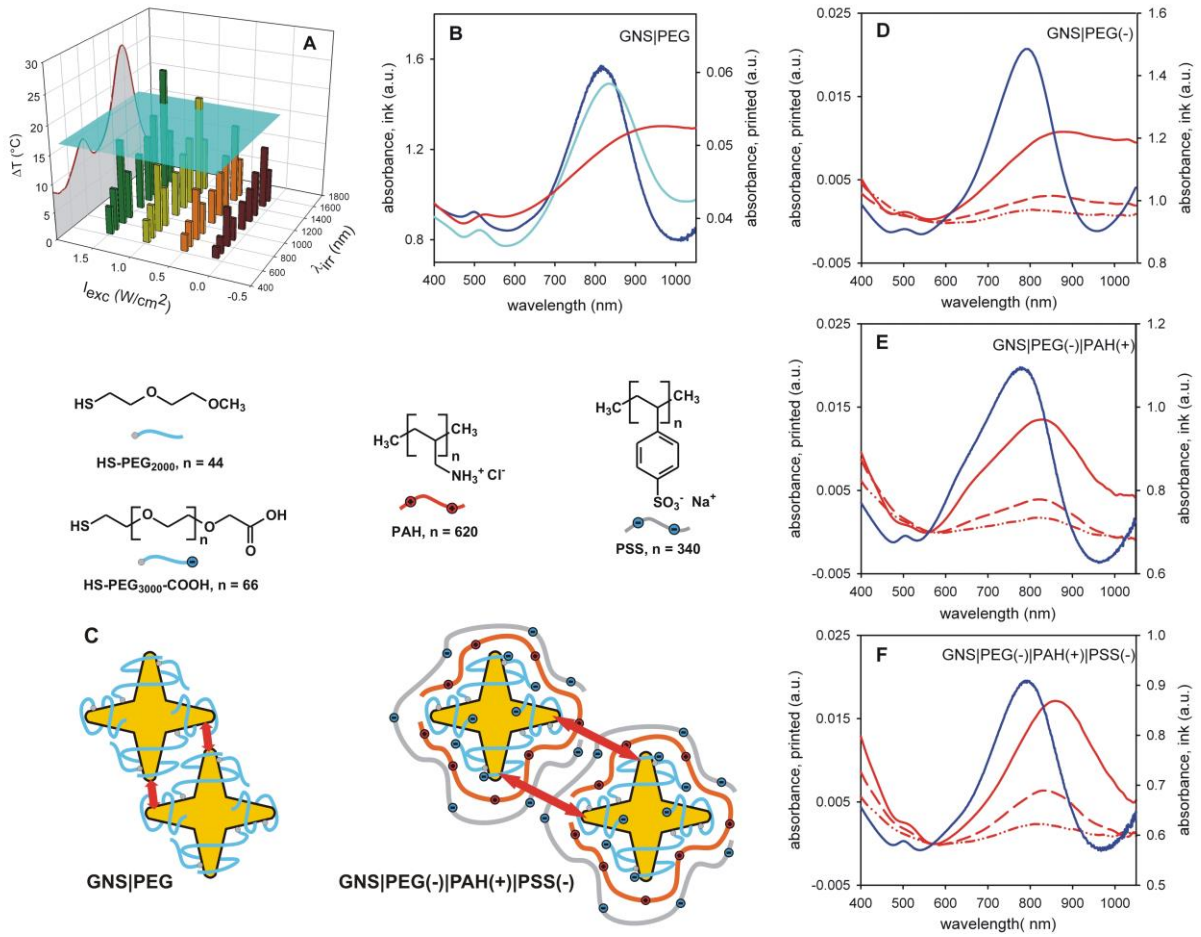

Figure 1. A: sketch of the photothermal response (ΔT) of a colloidal solution of GNS (vertical bars) as a function of λ_{irr} (irradiation wavelength) and of I_{exc} (fluence); the spectrum in the left back plane is a representative absorption spectrum of a GNS solution of the type reported in ref 12. **B:** absorption spectrum of a GNS ink contaning GNS|PEG (blue), of the same ink printed in glass (red) and of the printed pattern redissolved in water (azure). **C:** formula and sketch of the increase of the contact distance in printed patterns on stepping from pegylated GNS to GNS|PEG(-)|PAH(+)|PSS(-). D-F: absorption spectra of the liquid ink (blue) and of 2 (red, line-dot-dot), 5 (red, dashed), 11 (red solid) printed layers on glass, for GNS|PEG(-),GNS|PEG(-)|PAH(+) and GNS|PEG(-)|PAH(+)|PSS(-), respectively.

The absorption spectrum of the obtained blue-black dry GNS|PEG pattern was measured with a conventional absorption spectrophotometer, using a mechanical device for holding flat solid samples. The spectrum showed a huge red shift with respect to solution, with a dramatic overall broadening and loss of the peak structure, Figure 1B, red line. The printed layer can be redissolved in water, obtaining a blue-black solution displaying an absorption spectrum with a band shape almost identical to the ink solution, Figure 1B, cyan line, with regeneration of the starting GNS|PEG colloid. This indicates that the printing and drying processes have not caused a permanent aggregation (cohalescence) or modification of the GNS. The red shift and flattening of the LSPR band, resulting in an almost featurless absorption, is to be attributed to plasmon coupling between GNS, a phenomenon already described for other shapes of Au nanoparticles[20] and observed at short interparticle distances (< 10nm [21]). In printed conditions the GNS|PEG branches can be in close contact, since they are kept separated only by few nanometers by their thin PEG coating, as sketched in Figure 1C. The small thickness of a PEG coating on GNS was already revealed by DLS studies, showing that grafted HS-PEG_{2000} wraps around the GNS branches, causing a very small overall dimensional increase[22]. We have also prepared GNS|PEG coated with HS-PEG_{5000} (average mw 5000) but observed an identical broadening of the absorption spectrum on printing. This is detrimental in view of using GNS as the photothermal responsive component in an ink for secure writing. Consequently, we worked towards the increase of the coating thickness, with the aim of keeping GNS separated enough in the printed patterns to avoid plasmon coupling. This was pursued by enveloping GNS in successive layers of ionic polymers, adhering to GNS by electrostatic attraction with the opposite charge. We used the positive polymer PAH (polyallylamine hydrochloride) and the negative polymer PSS (polystyrene sulphonate), see Figure 1C, that have been reported to add 2.2 nm thickness for each layer around Au nanoparticles[23] and GNS.[19] We first coated GNS with the negatively charged HS-PEG_{3000}-COOH (mw = 3000, Figure 1C, -COOH groups deprotonate at pH 7), obtaining GNS|PEG(−). A PAH layer was then added to obtain GNS|PEG(−)|PAH(+)

and a further PSS overlayer gave GNS|PEG(−)|PAH(+)|PSS(−), sketches in Figure 1C, coating and purification procedures in the SI. The obtained aqueous colloidal solutions of GNS|PEG(−), GNS|PEG(−)|PAH(+) and GNS|PEG(−)|PAH(+)|PSS(−) had concentrations of 0.56, 0.42 and 0.36 mg Au/mL, respectively, as determined by ICP-OES (SI). To prepare a printable ink, these solutions were diluted 2:1 v/v with 2-propanol. The three inks were printed on glass slides using the same parameters as for GNS|PEG, printing 1x1 cm patterns with multiple (2-11) printed layers.

The absorption spectra of the printed squares were recorded. Beside the expected increased absorption with the number of printed layers, we observed (Figure 1D) that, as found for GNS|PEG, the printed GNS|PEG(−) ink shows a red-shifted and broadened absorption spectra, red curve, with respect to the parent ink solution, blue curve. On the other hand, printed GNS|PEG(−)|PAH(+) and even better printed GNS|PEG(−)|PAH(+)|PSS(−) displayed adsorption spectra that were red shifted but maintained the desired peak-like shape (red curves, Figure 1 E and F, respectively). SEM inspection of the printed patterns showed that GNS|PEG(-) crop in isles (dimensions < 1μm) on the printed glass surface, see **Figure 2**A**,** in agreement with the hypotyhesized contact of GNS resulting in plasmon coupling and band flattening. As similar microstructures are observed also for GNS|PEG(-)|PAH(+) and GNS|PEG(-)|PSH(+)|PSS(-) printed patterns (see SI), the sharper absorption bands obtained with these GNS inks are to be attributed to the increase of their coating layer thickness and larger interparticle separation, see sketch in Figure 1C. We tried to investigate the thickness of the coating layer by transmission electron microscopy (TEM). Imaging a non-cristalline thin layer of soft and atomically light polymeric matter on a Au nanoparticle is a difficult task due to two diverse effects. First, the likely beam sensitivity of the polymer, which could give rise to partial or total destroying of the thinnest part of the polymer due to radiolysis. Second, even if a polymer external layer is present, the very high difference in contrast between the GNS and the thinnest part of their surrounding polymeric layer could mask the latter one. However, even if in Figure 2B the PEG(-) layer

around the GNS looks not detectable, the TEM images reported in Figure 2C-D for GNS|PEG(-)|PAH(+) and GNS|PEG(-)|PSH(+)|PSS(-), respectively, support the hypothesis of an increasing thickness of the coating layer. A layer is in fact visible where it appears thick enough, in correspondence of the central part of the GNS in Figure 2C-D, as evidenced by the red arrows.

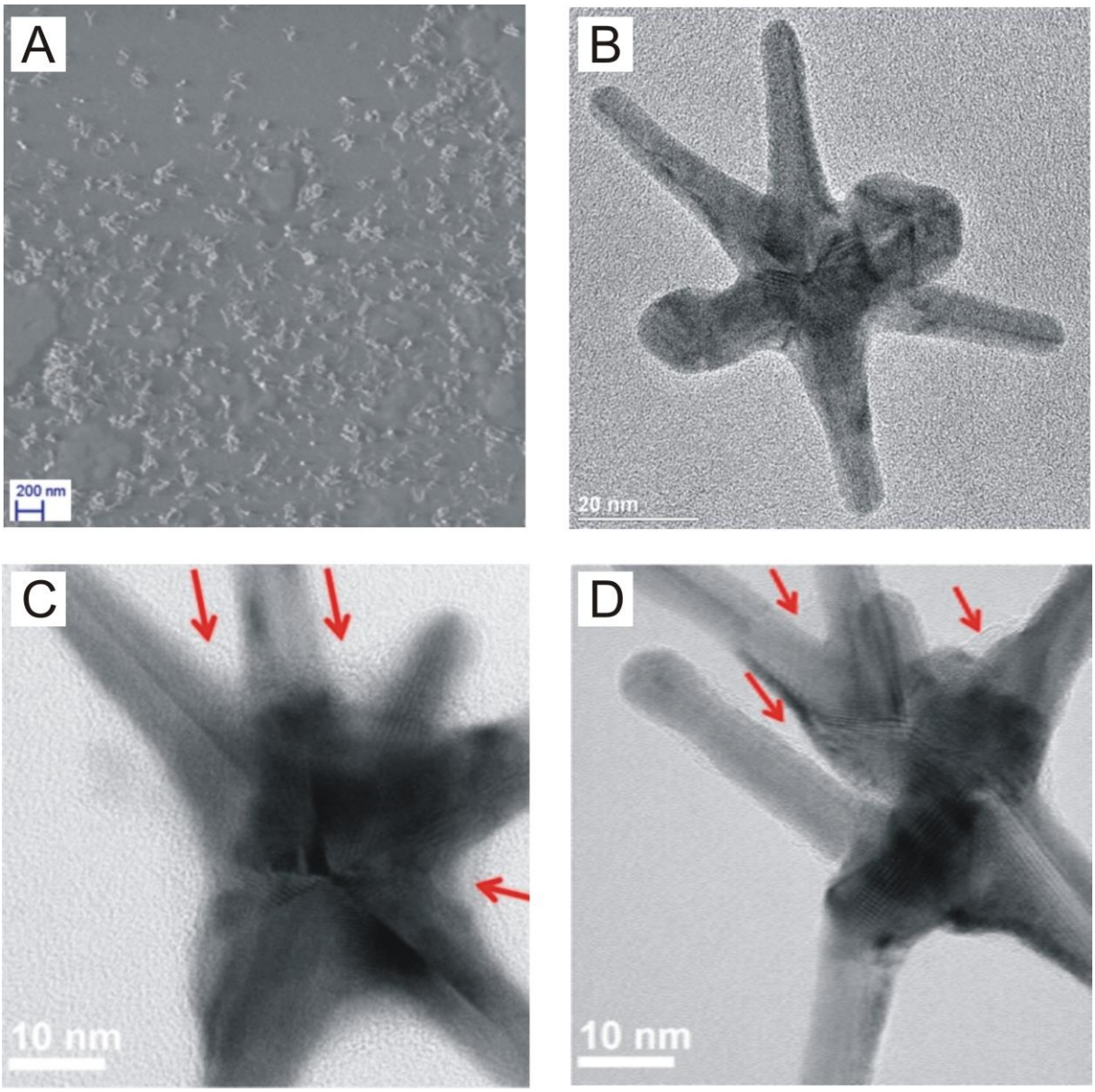

Figure 2. Scanning and Transmission Electron Microscopy (SEM and TEM) images. Panel A: SEM inspection (mag 50k) of the printed patterns shows that for GNS|PEG(-) crop in isles (dimensions < 1μm) on the printed glass surface. Panels B-D are high magnifcation TEM images of single GNS|PEG(-), GNS|PEG(-)|PAH(+) and GNS|PEG(-)|PSH(+)|PSS(-) particles, respectively. The red arrows indicate the evidence of the polymeric coating.

The photothermal response of the printed GNS inks was examined using a set of laser sources with λ_{irr} at 730, 800, 850, 890, 940, 1064, with I_{exc} (irradiance) between 0.16 and 0.8 W/cm^2. To

carry on a proof of concept study on secure writing we choose the patterns with 11 printed layers, as larger T increases are observed. We used a thermocamera reading a ROI (Region Of Interest) of 320x240 pixels inside the irradiated area. We observed a steep ascending T kinetics for all λ_{irr}, with a roll-off to a plateau value in less than ≈10 s (see ESI). The thermal response read in the ROI under laser interrogation is $\Delta T = T(plateau) - T(room)$. Significantly for our aims, at a given I_{exc} the observed ΔT vs λ_{irr} follows the absorption profiles, as it is shown in **Figure 3**, top graphs, for $I_{exc} = 0.8$ W/cm^2. Moreover the trend of ΔT as a function of I_{irr} is linear in a wide range of values (Figure 3G, M).

These data fit the simple concept of secure writing described in Figure 1A: if the threshold ΔT is e.g. 20 ^{o}C, only the GNS|PEG(-)|PSH(+)|PSS(-) pattern would give a YES answer and only if interrogated at λ_{irr} = 890 and 900 nm with $I_{exc} = 0.8$ W/cm^2. However, more complex reading schemes can be envisaged. In particular the GNS|PEG(-)|PSH(+)|PSS(-) ink offers wider possibilities, thanks to the sharp peaked nature of its ΔT vs λ_{irr} response (Figure 3C). An absolute and a relative scheme can be devised by working e.g. on the maximum (λ_{irr} = 890 nm) and minimum (λ_{irr} = 1064 nm) ΔT values. If the effective irradiance on the sample was known, an absolute threshold could be set, ΔT_{thr}, then asking if the temperature reading on a pattern satisfies the conditions: $\Delta T_{890}/\Delta T_{thr} \geq 2$ AND $\Delta T_{1064}/\Delta T_{thr} \geq 1$. As an example, if ΔT_{thr} = 10 °C is chosen (Figure 3D, E and F), only the pattern printed with GNS|PEG(-)|PSH(+)|PSS(-) ink (Figures 3**C** and F) would give a YES answer (double black boxes, AND logic test).

However, this reading scheme can be affected by the uncertainty on the source irradiance. As a more robust alternative, one can define a normalized temperature signature $S=(\Delta T_{890}-\Delta T)/\Delta T_{890}$, and set a three (or multiple) levels multi-wavelength test. As an example, the conditions could be chosen as follows:

$S(\lambda_{irr}) \geq 0.4$ barcode $=B(\lambda_{irr}) = 3$ (black)

$0.4 > S(\lambda_{irr}) \geq 0.2$ barcode $= B(\lambda_{irr}) = 2$ (gray)

$0.2 > S(\lambda_{irr})$ barcode = $B(\lambda_{irr}) = 1$ (white)

This conditional test can be run on each of the N_λ sampled wavelengths $\{\lambda_i\}_{i=1..N\lambda}$, providing a three color bar code $\{B(\lambda_i)\}_{i=1,..N\lambda}$ with a number of bars equal to the number N_λ of read wavelengths. In the cases reported in Figure 3H, I, L the printed patterns give different bar codes. It is noteworthy that, due to the linear dependence of ΔT on the source irradiance (Figure 3G and M), the temperature signature S does not depend on the source irradiance, making the reading scheme much more robust for practical implementations.

The presence of an intrinsic uncertainty in the photothermal response calibration may imply uncertainty in the bar code output, especially if a single interrogation is used. This does not prevent the possibility to discriminate between the three different patterns. If we assume that the reference pattern is the one printed with the GNS|PEG(-)|PSH(+)|PSS(-) ink (Figure 3L, $\{B_{ref}(\lambda_i)\} = \{3,2,1,2,3\}$), we can evaluate a matching score with the other two patterns by computing the root mean square (rms) value of the difference of the temperature signature between the read pattern and the reference one. We can define it as:

$$(S_{rms})^2 = \Sigma_i [(B_{ref}(\lambda_i) - B(\lambda_i))/(B_{ref}(\lambda_i) + B(\lambda_i))]^2$$

For the given example, the S_{rms} score is only 45% for the pattern printed with GNS|PEG(-). The score raises to 61% - 66%, for the pattern printed with the GNS|PEG(-)|PAH(+) ink. It is noteworthy that the uncertainty in the thermo-imaging reading (solid and dashed lines in Figure 3H,I, L) result only in a 4% variability of the scores, that are in any case well discriminated from the reference one, $S_{rms} = 1$ ($p \leq 0.02$). This suggests that such an approach may be suitable for printing a new type of anti-counterfait signatures on goods of eg commercial, military or medical use.

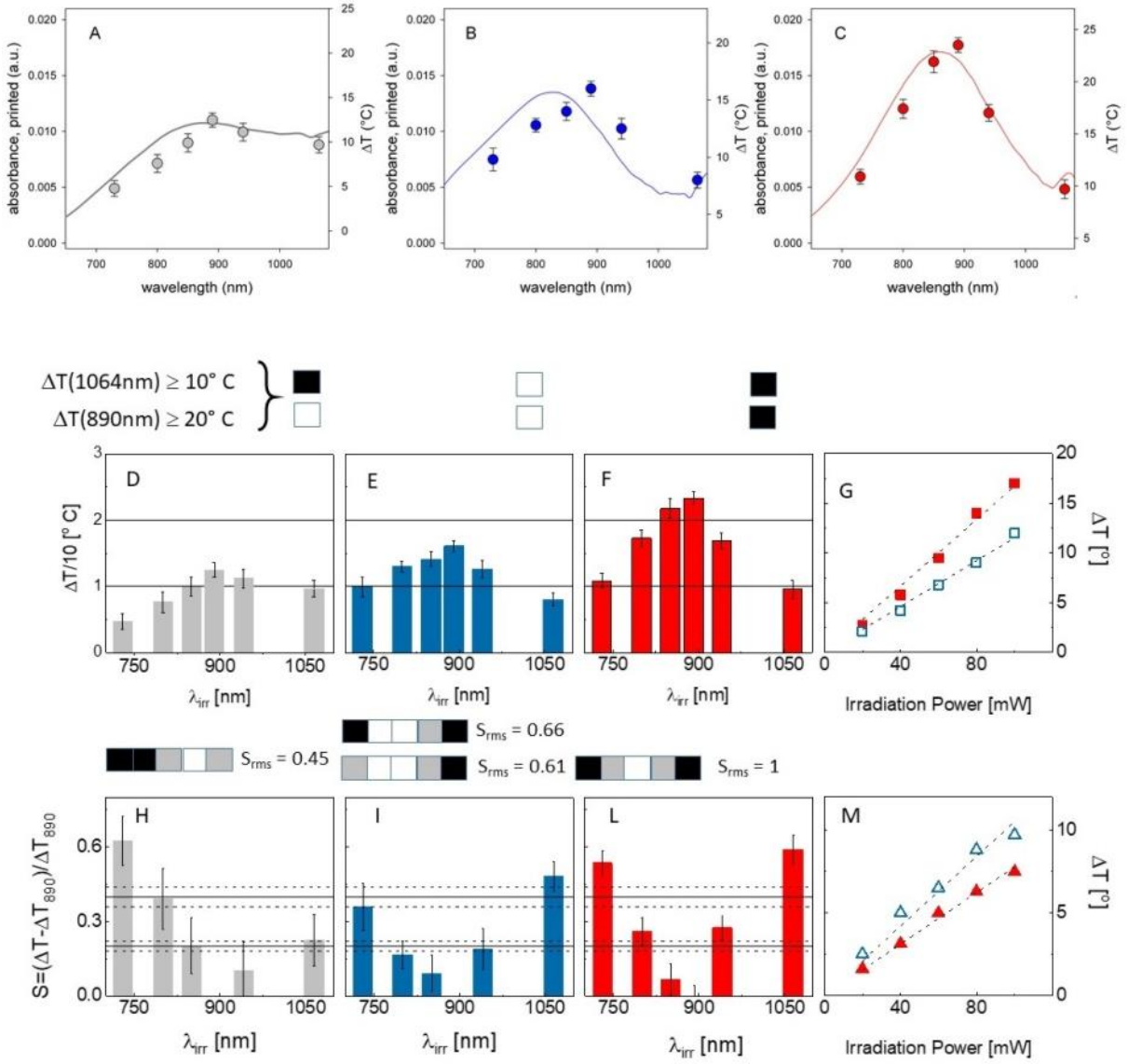

Figure 3. Photothermal efficiency, ΔT, of printed patterns and possible reading methods. The panels A, B and C report the temperature increase or patterns printed with GNS|PEG(-) (gray), GNS|PEG(-)|PAH(+) (blue) and GNS|PEG(-)|PSH(+)|PSS(-) (red), respectively, as a function of the irradiation wavelength (I_{exc} = 0.8 W/cm^2). The solid lines represent in each panel the corresponding extinction spectrum. The panels D, E, F report the temperature increase normalized to 10 °C. The panels H, I, L report the temperature signature defined as $S=(\Delta T-\Delta T_{890})/\Delta T_{890}$. Panels G and M reports the trend of ΔT as a function of the irradiation power for λ_{irr} = 800 nm (G) and λ_{irr} = 1064 nm (M). In each panel the hollow blue and filled red symbols refer to GNS|PEG(-)|PAH(+)and GNS|PEG(-)|PSH(+)|PSS(-), respectively.

Finally, also the quantity of Au printed in a surface unit is a relevant parameter that influences the ΔT response and may thus be used as a further key to encode the correct thermal answer in a printed pattern. The mass of Au/cm^2 is tuned by the ink concentration and by printing parameters such as drop volume, drops spacing, number of printed layers. The detailed investigation of the interplay of these parameters on the thermal response of a GNS printed pattern is currently under

study and out of the aims of this communication. Our preliminar data (not shown) indicate that by increasing the number of printed layers the dependence of ΔT on the Au/cm^2 becomes sublinear. This non-linearity, which could be easily modeled by taking into account inner filtering effects,[11] would add additional power to the proposed counterfeit method.

In conclusion we have prepared inks based on GNS that printed in a 2D pattern maintain the same peaked Abs vs λ spectrum as in solution, corresponding to a similarly peaked ΔT vs λ_{irr} profile. This allows to print secure informations that are not read visually but through encoding schemes of increasing complexity: i) $\Delta T > T$ threshold at a single λ_{irr} for a given single I_{exc}; ii) generation of a thermal barcode by multiple λ_{irr} interrogation; iii) evaluation of the authenticity of a printed pattern by checking the matching score of a thermal barcode with a reference pattern. We believe that this may be the first step towards a wide range of applications that include highly-technological labelling, hiding secure information on public surfaces, reading information in the dark, remote recognition using non-visible signals. All these issues have important societal impacts, from avoiding brands falsification to understanding the nature, origin and reliability of a vehicle from a safety distance.

Supporting Information

Supporting Information is available from the Wiley Online Library or from the author.

Acknowledgements

The research project "Photothermally responsive inks for inkjet-printing secure informations" has been granted by Università di Pavia, Blue Sky Research 2017 (BSR1774514).
Colm O'regan acknowledges financial support received from the King Abdullah University of Science and Technology (KAUST) baseline funding of Prof. Andrea Falqui.
Thanks are due for SEM imaging to Prof. Emilano Fratini and CSGI, Department of Chemistry "Ugo Schiff", Università di Firenze, Italy

Received: ((will be filled in by the editorial staff))
Revised: ((will be filled in by the editorial staff))
Published online: ((will be filled in by the editorial staff))

References

[1] M. Singh, H.M. Haverinen, P. Dhagat, G. E. Jabbour, *Adv. Mater.* **2010**, *22*, 673.

[2] E. Tekin, P.J. Smith, U.S. Schubert, *Soft Matter* **2008**, *4*, 703.

[3] H.Tao, B. Marelli, M. Yang, B. An, M. Serdar Onses, J.A. Rogers, D.L. Kaplan, F.G. Omenetto, *Adv. Mater.* **2015**, *27*, 4273.

[4] A.K. Määttänen, D. Fors, S. Wang, D. Valtakari, P. Ihalainen, J. Peltonen, *Sens. Actuators, B* **2011**, *160*, 1404.

[5] X. Cui, T. Boland, D.D. D'Lima, M.K. Lotz, *Recent Pat. Drug Delivery Formulation* **2012**, *6*, 149.

[6] C.E. Krause, B.A. Otieno, A. Latus, R.C. Faria, V. Patel, J.S. Gutkind, J.F. Rusling, *ChemistryOpen* **2013**, *2*, 141.

[7] P. Ihalainen, F. Pettersson, M. Pesonen, T. Viitala, A. Määttänen, R, Österbacka, J. Peltonen, *Nanotechnology* **2014**, *25*, 094009.

[8] A. Doraiswamy, T.M. Dunaway, J.J. Wilker, R.J. Narayan, *J. Biomed. Mater. Res., Part B* **2009**, *89*, 28.

[9] J. Jalo, H. Sillanpaa, R.M. Makinen, *Prog. Electromagn. Res.* **2013**, *142*, 409.

[10] S. Gamerith, A. Klug, H. Scheiber, U. Scherf, E. Moderegger, E.J. List, *Adv. Funct. Mater.* **2007**, *17*, 3111.

[11] M. Borzenkov, A. Määttänen, P. Ihalainen, M. Collini, E. Cabrini, G. Dacarro, P. Pallavicini, G. Chirico *ACS Appl. Mater. Interfaces* **2016**, *8*, 9909−9916.

[12] P. Pallavicini, A. Donà, A. Casu, G. Chirico, M. Collini, G. Dacarro, A. Falqui, C. Milanese, L. Sironi, A. Taglietti, *Chem. Commun.* **2013**, *49*, 6265.

[13] A. Casu, E. Cabrini, A. Donà, A. Falqui, Y. Diaz-Fernandez, C. Milanese, A. Taglietti, P. Pallavicini, *Chem. Eur. J.* **2012**, *18*, 9381.

[14] G. Dacarro, P. Pallavicini, S. M. Bertani, G. Chirico, L. D'Alfonso, A. Falqui, N. Marchesi, A. Pascale, L. Sironi, A. Taglietti, E. Zuddas, *J. Colloid Interface Sci.* **2017**, *505*, 1055.

[15] S. Link, M.A. El-Sayed, *Int. Rev. Phys. Chem.* **2000**, *19*, 409.

[16] P.K. Jain, X.H. Huang, I.H. El-Sayed, M.A. El-Sayed, *Acc. Chem. Res*. **2008**, *41*, 1578.

[17] F. Jabeen, M. Najam-ul-Haq, R. Javeed, C.W. Huck, G.K. Bonn, *Molecules* **2014**, *19*, 20580.

[18] P. Pallavicini, A. Donà, A. Taglietti, P. Minzioni, M. Patrini, G. Dacarro, G. Chirico, L. Sironi, N. Bloise, L. Visai, L. Scarabelli, *Chem. Commun.* **2014**, *50*, 1969.

[19] S. Freddi, L. Sironi, R. D'Antuono, D. Morone, A. Donà, E. Cabrini,L. D'Alfonso, M. Collini, P. Pallavicini, G. Baldi, D. Maggioni, G. Chirico, *Nano Lett.* **2013**, *13*, 2004.

[20] N.J. Halas, S. Lal, W.-S. Chang, S. Link, P. Nordlander, *Chem. Rev.* **2011**, *111*, 3913.

[21] S.-D. Liu, M.-T. Cheng, *J. Appl. Phys.* **2010**, *108*, 034313.

[22] P. Pallavicini, C. Bernhard, G. Chirico, G. Dacarro, F. Denat, A. Donà, C. Milanese, A. Taglietti, *Dalton Trans.* **2015**, *44*, 5652.

[23] A.E. El Haitami, D. Martel, V. Ball, H.C. Nguyen, E. Gonthier, P. Labbé, J.-C. Voegel, P. Schaaf, B. Senger, F. Boulmedais, *Langmuir*, **2009**, *25*, 2282.

Table of Contents entry

Photothermally responsive NIR absorbing Gold NanoStars are inkjet-printed in 2D patterns. Proper GNS coating avoids LSPR coupling after printing, with ΔT vs $\lambda_{irradiation}$ profiles superimpoising to LSPR bands. A new paradigm for inkjet-printing secure information is introduced: while different printed patterns of GNS are visually indistinguishable, their photothermal response allows to write and thermally read barcodes and anti-counterfait signatures

Keyword: photothermal secure information

G. Chirico, G. Dacarro, C. O'Regan, J. Sarfraz, A. Taglietti, M. Borzenkov,* and P. Pallavicini*

Photothermally responsive inks for inkjet-printing secure information